Supplementary Materials: Improved Recovery and Selectivity of Lanthanide-Ion-Binding Cyclic Peptide Hosts by Changing the Position of Acidic Amino Acids

Yoichi Hosokawa *, Ayako Oshima, Takaaki Hatanaka and Nobuhiro Ishida *

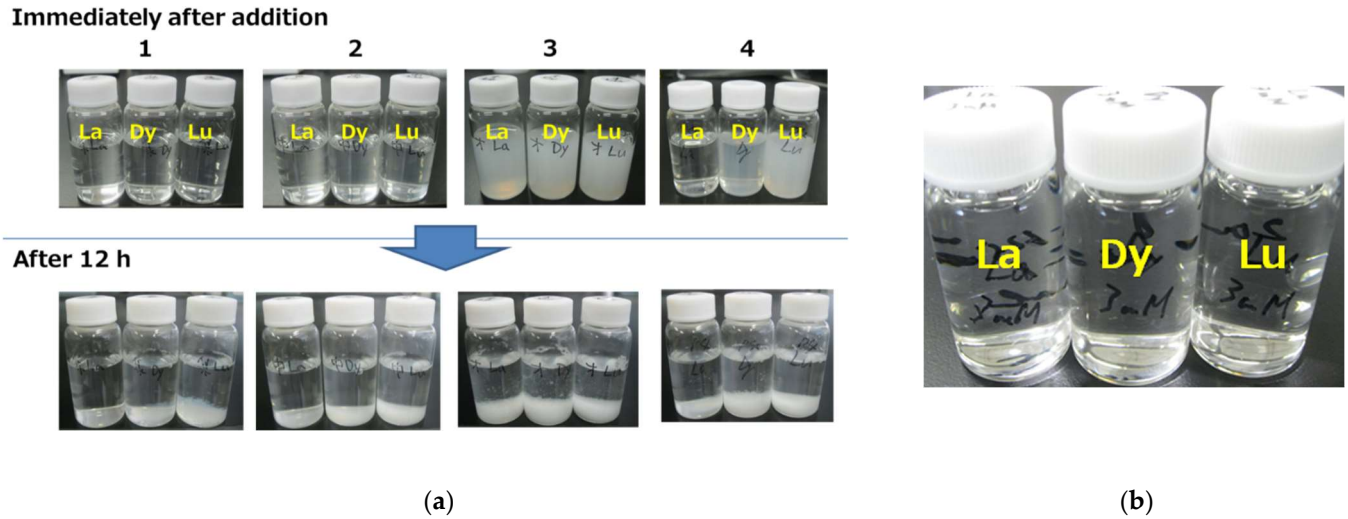

Figure S1. Photographic images of the reactions of precipitate by model peptides. (**a**) Images immediately after the reaction and 12 h later. (**b**) Ln control solutions without peptides after 1 month.

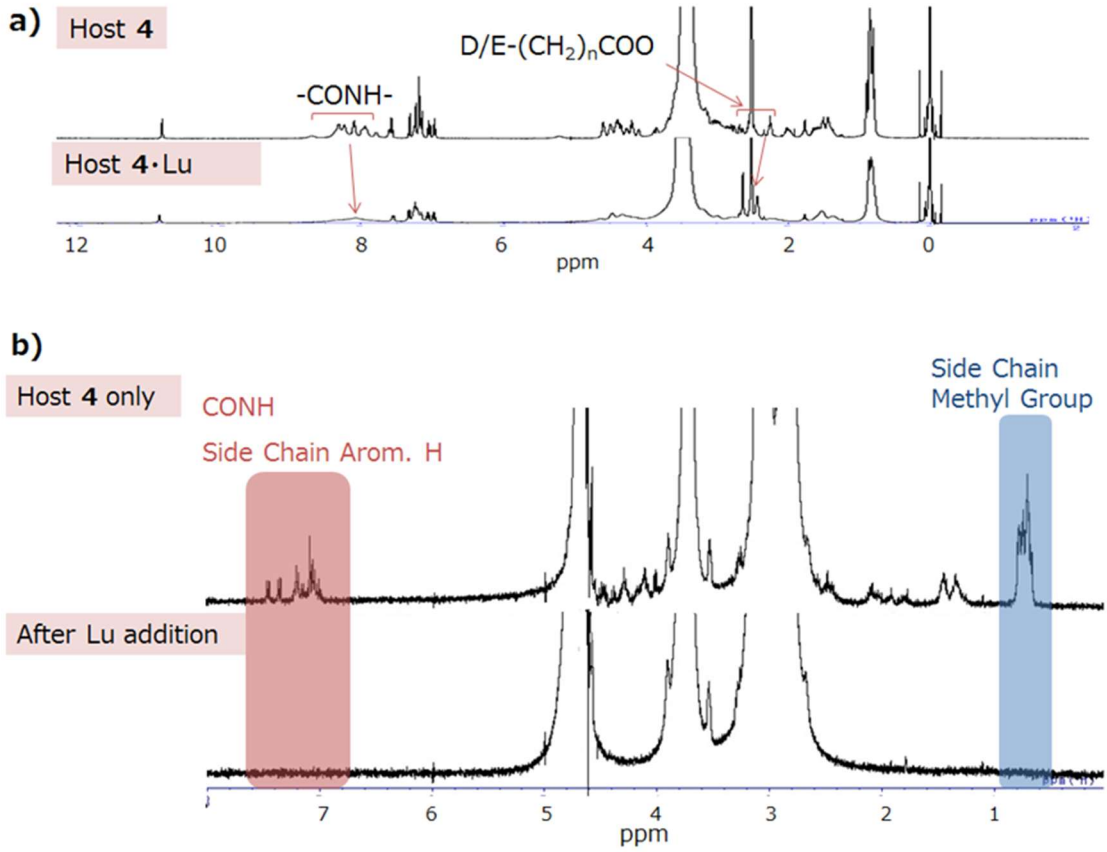

Figure S2. ^{1}H NMR spectra of (**a**) host **4** and its Lu precipitate, and (**b**) the reaction solution before (host **4** only) and after Lu addition (400 MHz, DMSO-d6).

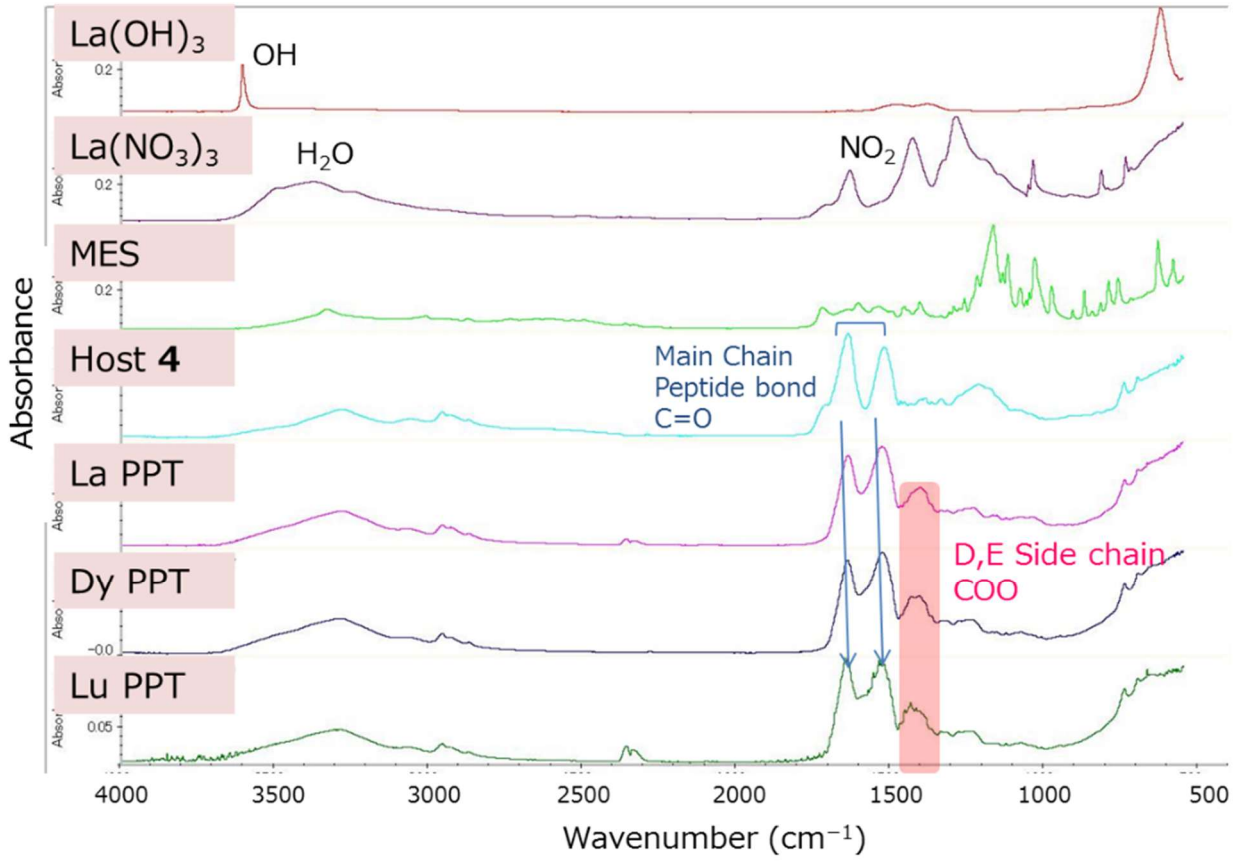

Figure S3. ATR-FTIR spectra of host **4** and its precipitates (PPTs), and spectra of related compounds (La salts, MES) for comparison.

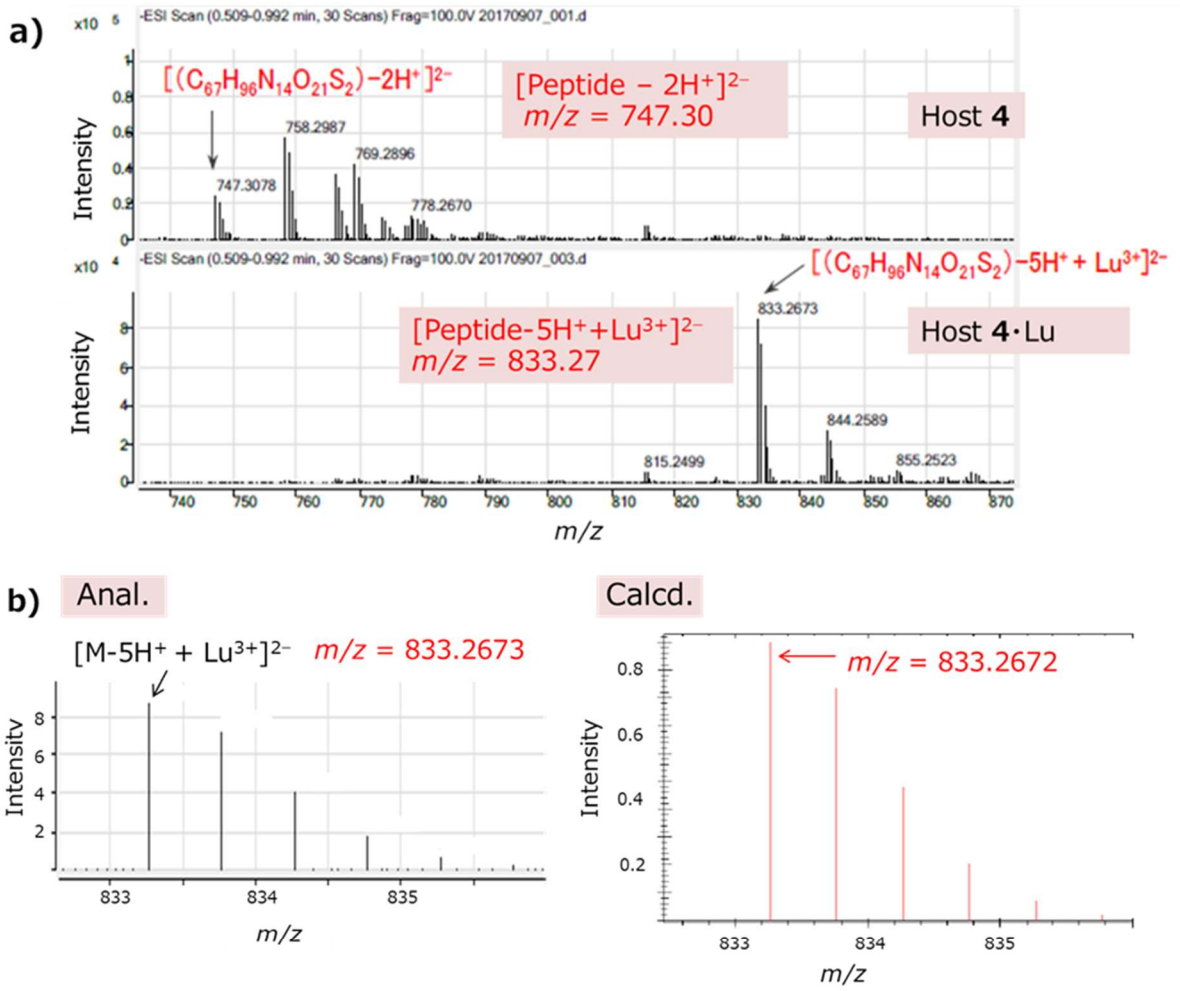

c)

Precipitation		Molecular Ion Observed	*m/z*
Host **4**	La	$[M-5H^+ + La^{3+}]^{2-}$	815.2532
	Dy	$[M-5H^+ + Dy^{3+}]^{2-}$	827.7651
	Lu	$[M-5H^+ + Lu^{3+}]^{2-}$	833.2697

Figure S4. (**a**) ESI-MS spectra of host **4** and its precipitate with Lu (**4**·Lu). (**b**) Enlarged molecular-ion peak of host **4**·Lu. (**c**) Summary of the observed molecular-ion formula of the precipitates of host **4** with Ln ions (La, Dy, and Lu).

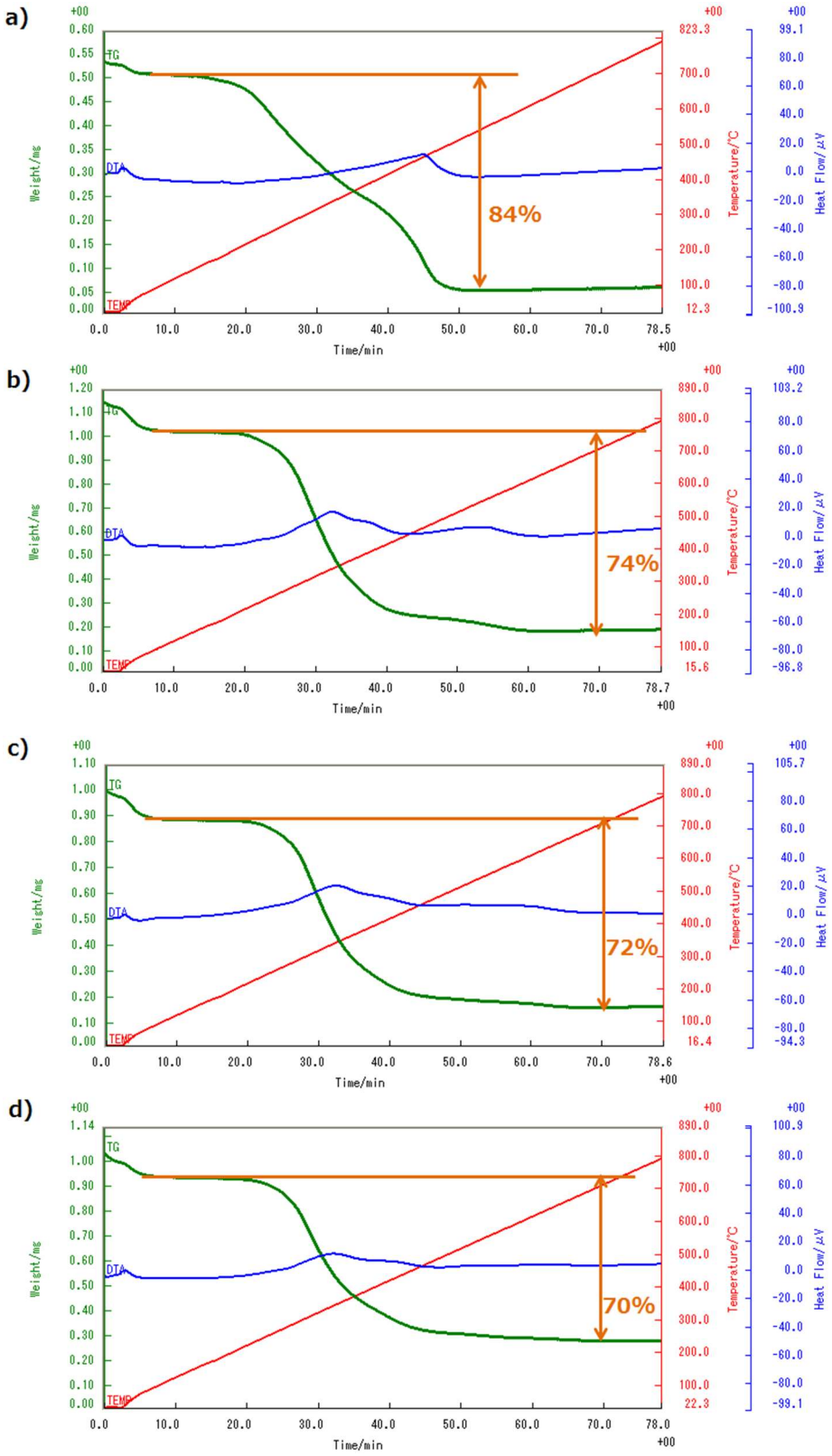

Figure S5. TG-DTA charts of a) host **4** and its precipitates with b) La (**4**·La), c) Dy (**4**·Dy), and d) Lu (**4**·Lu). Green: TG (weight / mg). Blue: DTA (heat flow / μV). Red: Temperature (temperature / °C).

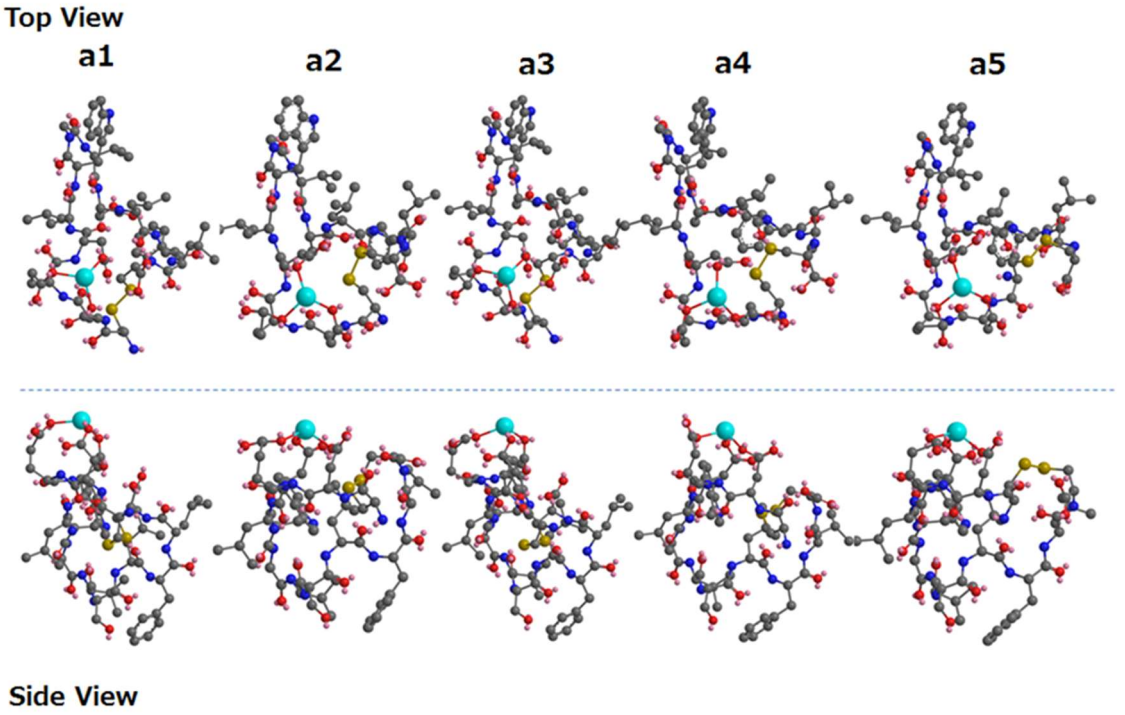

Figure S6. MM2 optimized structure of **a1-5** in Figure 4.

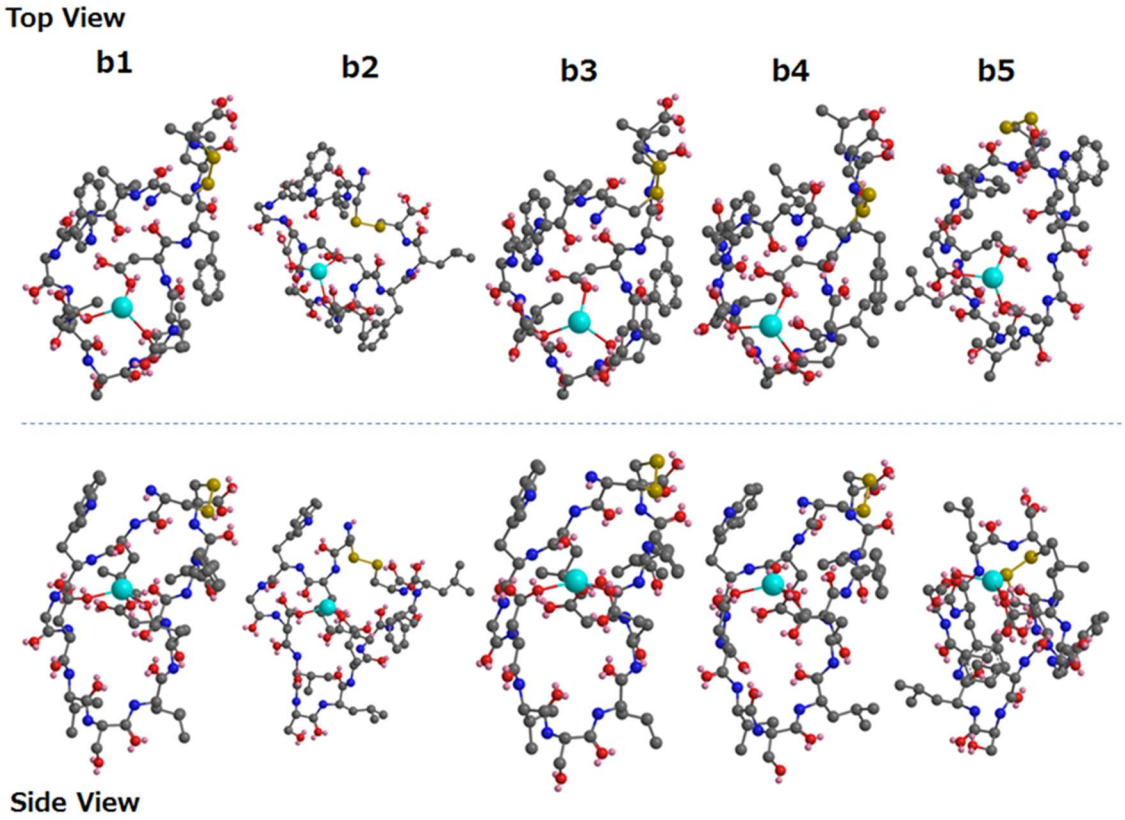

Figure S7. MM2 optimized structure of b1-5 in Figure 4.

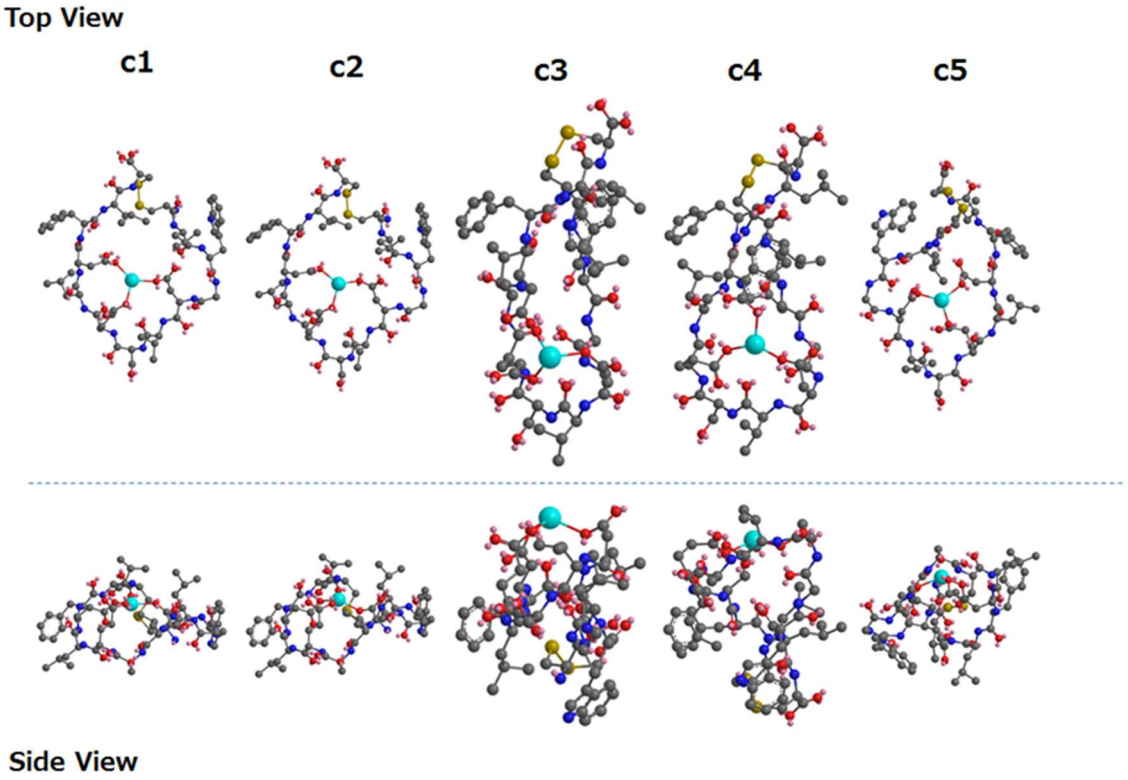

Figure S8. MM2 optimized structure of **c1**-**5** in Figure 4.

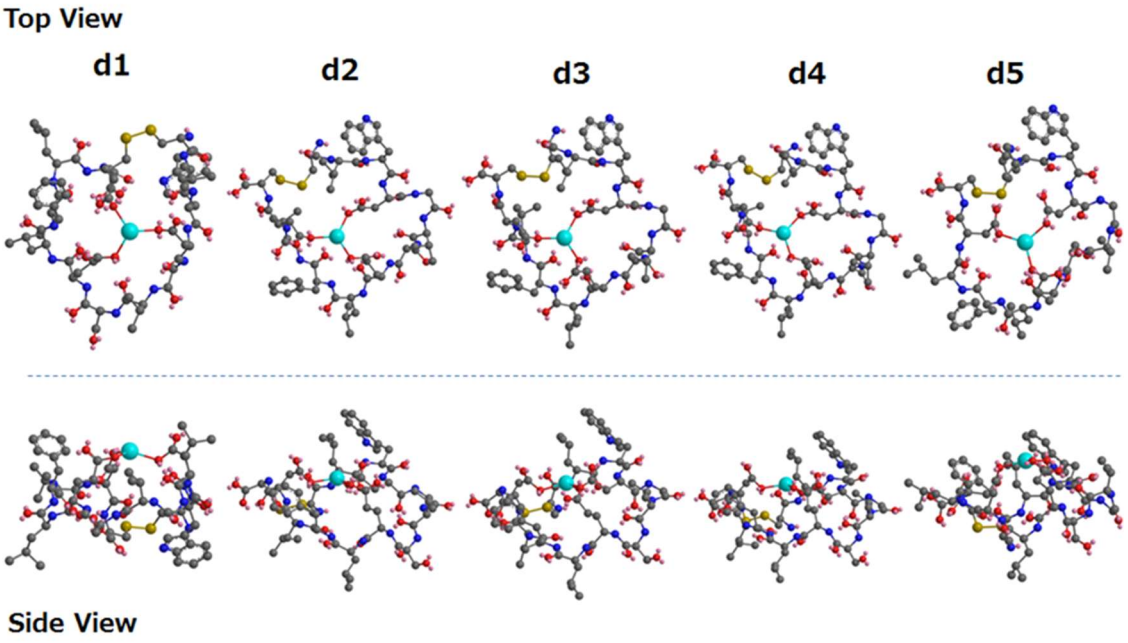

Figure S9. MM2 optimized structure of **d1**-**5** in Figure 4.

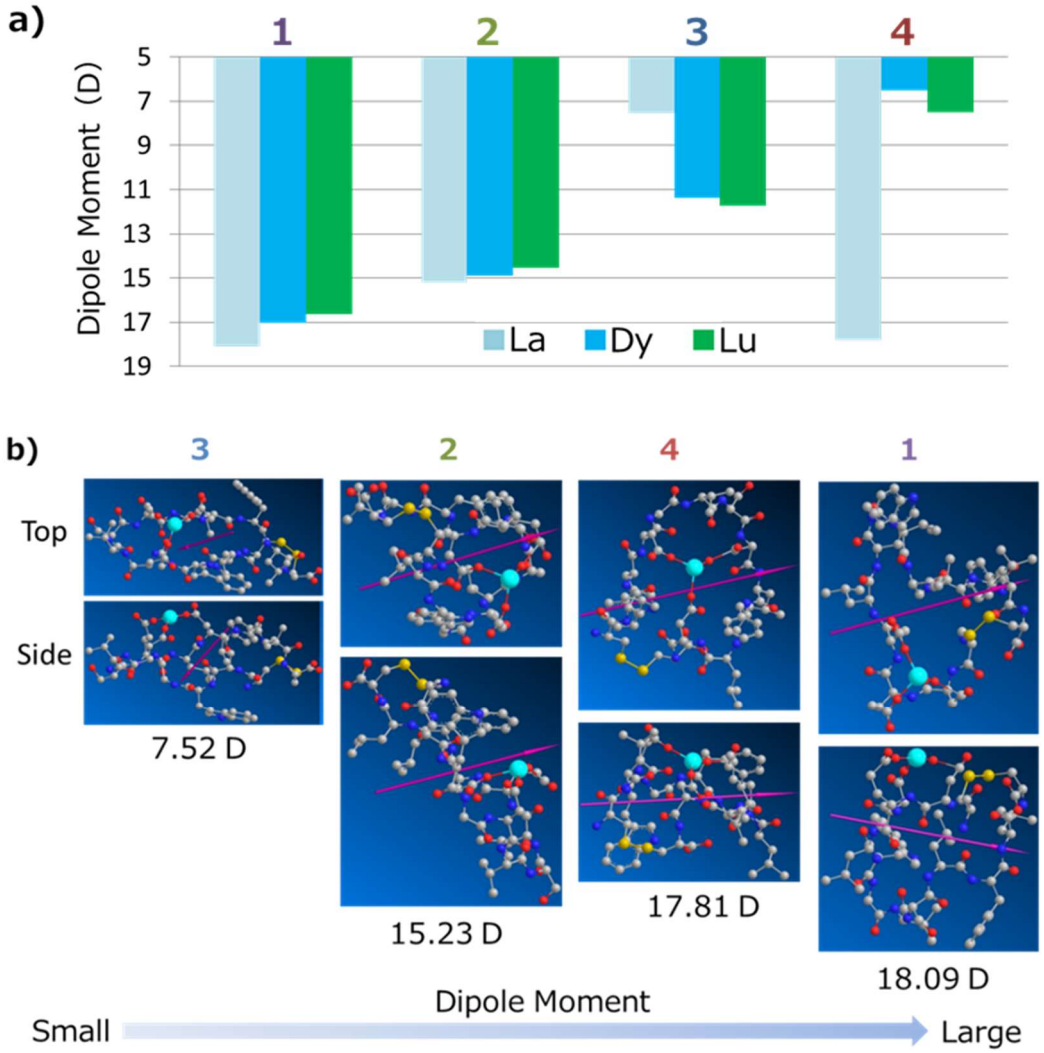

Figure S10. (**a**) DM of each host·Ln complex. (**b**) DM vector and optimized structure of each host·La complex, as representative results.

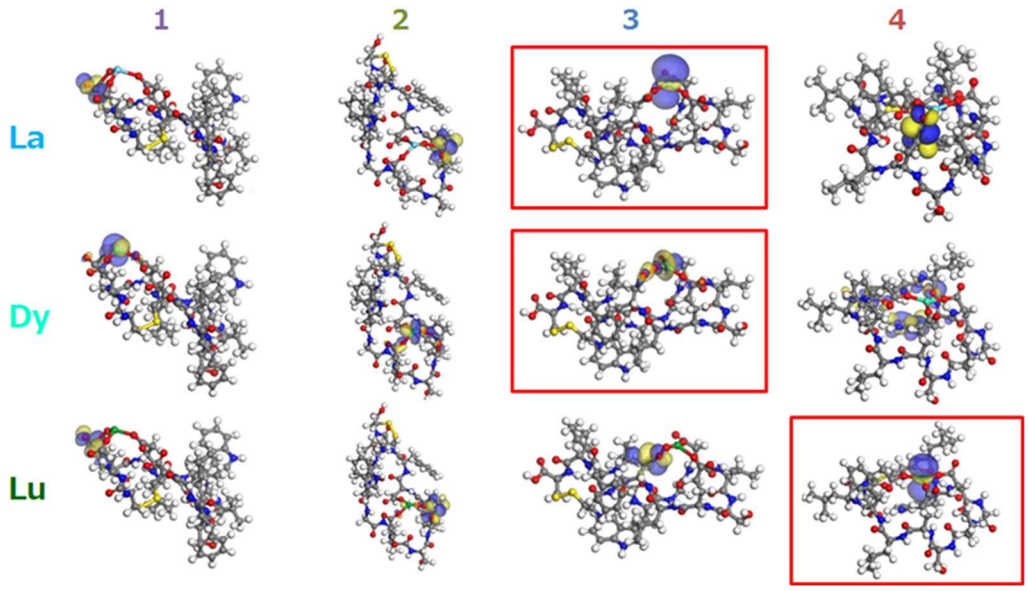

Figure S11. LUMO orbital of each host·Ln complex. Complexes with the LUMO centered on the metal element are shown in red boxes.

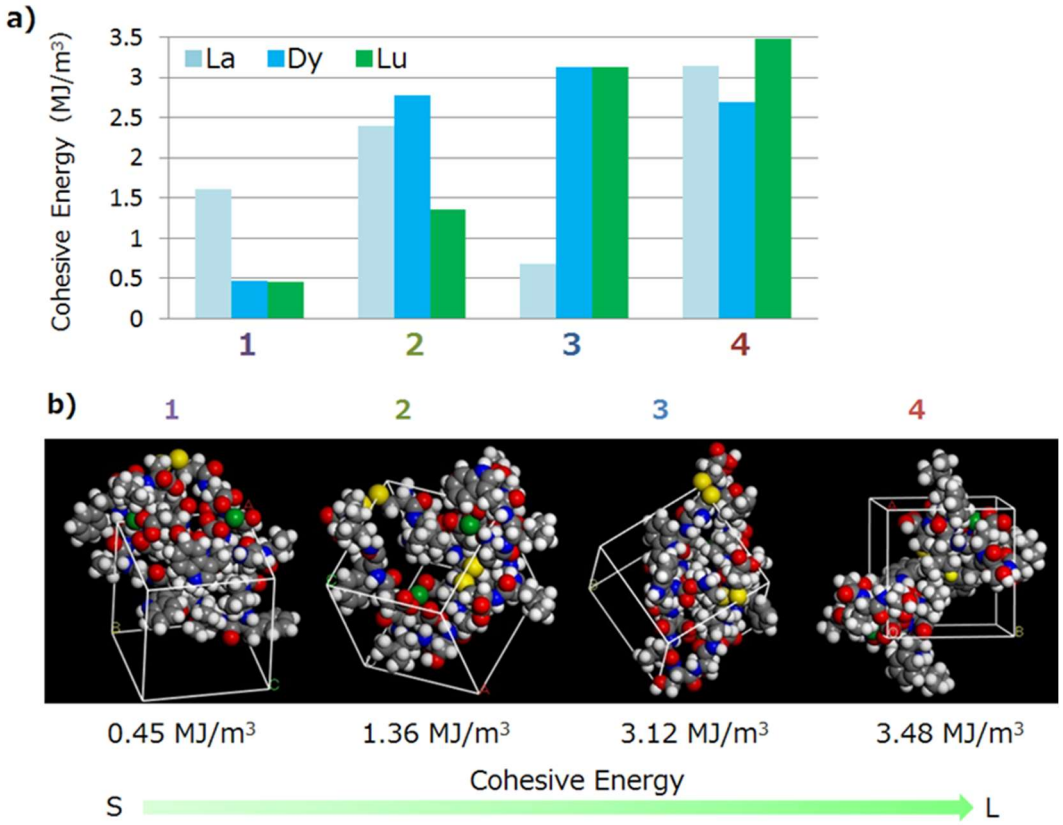

Figure S12. Cohesive energy of each host·Ln complex. (**a**) Bar graph and (**b**) cohesive structure of each host·Lu complex, as representative results.

Table S1. TG-DTA analysis data of host **4** and its precipitate with each Ln complex (Figure S7).

Compound	Initial Weight (mg)	Final Weight (mg)	Weight Loss (%)	
			Anal (Temp. Range/℃)	Calcd
Host **4**	0.512	0.052	84.27 (100 - 550)	-
Host **4**·La	1.03	0.180	74.01 (120 - 700)	74.31
Host **4**·Dy	0.894	0.157	72.70 (120 - 700)	72.84
Host **4**·Lu	0.946	0.282	70.20 (120 - 700)	72.11

Table S2. Isolated yield (%) of each host·Ln complex.

	Host 1	Host 2	Host 3	Host 4
La	1	1	41	11
Dy	3	6	57	40
Lu	6	12	81	99

Table S3. ICP-OES yield (%) of each host·Ln complex.

	Host 1	Host 2	Host 3	Host 4
La	1	1	35	19
Dy	0	2	46	26
Lu	16	20	78	97

Table S4. Total energy (kcal/mol) of each host·La complex as determined by MM2 calculations.

La complex Structure	Host 1	Host 2	Host 3	Host 4
1	−31.8	85.5	44.2	−47.4
2	76.1	−41.2	−6.4	−27.3
3	41.9	−11.5	−23.2	−27.4
4	5.4	−21	−24	−27.2
5	68.7	−27.8	−19.1	−38.8

Table S5. Re-calculated YD (Left) and YC (Right) using each approximate curve in Figure 6A and 6B.

YD	Host 1	Host 2	Host 3	Host 4
La	0	26	96	2
Dy	9	29	61	100
Lu	13	32	58	96

YC	Host 1	Host 2	Host 3	Host 4
La	1	11	0	55
Dy	0	27	54	22
Lu	0	0	53	100

Table S6. Simulated yield of each host·Ln complex.

	Host 1	Host 2	Host 3	Host 4
La	0	9	48	14
Dy	2	14	57	37
Lu	3	8	28	98